Local Analysis of Individual-based Viral Dynamic Models with Eigenspace and Eigenvalue Elasticity Analysis

Qian Zhang*, Nathaniel Osgood†

Abstract

Eigenvalue elasticity methods have been widely applied in analyzing linear and simple nonlinear systems. In this study, we applied this approach to gain insight into the leverage offered by parameter changes in individual-based viral dynamic models for studying and controlling infectious disease spread. We found that such eigenspace based methods encounter severe limitations when applied to nonlinear systems with a relatively large number of state variables. Although eigenvalue elasticity offers some insight into the short-term impact of parameter changes, eigenvalue elasticity method can be complicated and even unwieldy for understanding the impacts of parameter changes for models with a relatively large number of state variables because of eigenvalue multiplicity, co-effects of eigenvalues, eigenvectors and coefficients. In terms of disease control, while such analysis methods could be helpful for identifying policy levers with high short-term impact, it is inefficient. In addition, we found that parameter changes guided by such local techniques are usually insufficient to alter system behaviors in the long-term, such as in the phase of endemic spread in the infectious disease spread. We argue that further work should be focused on refining eigenspace techniques and developing global analysis method to understand the impact of parameter changes on long-term behavior.

1 Introduction

Infectious diseases exhibit complex dynamic behaviors (e.g., sudden outbreak, oscillations, periods of quiescence, sudden die off) [1], and respond to control measures in complex and sometimes unexpected ways. These complexities can render some well-intentioned policies ineffective, and

---

*Department of Informatics, Indiana University, 919 E10th Street, Bloomington, IN, USA, 47408 ✉

†Department of Computer Science, University of Saskatchewan, 176 Thovaldson Building, 110 Science Place, Saskatoon, SK, Canada, S7N5C9 ✉

complicated policy choices. For this reason, dynamic models have long been used to capture complexities and hidden dynamic characteristics and structures of outbreaks, spread, and impacts of policies.

In this paper, we focus on a relatively new type of infectious diseases spread model, which combines individual-based models and immunological dynamic models, to establish a relatively detailed "immuno-epidemiological" dynamic model. We seek to use analytic techniques to better understand the dynamics of such models during disease outbreaks. Specifically, by applying local techniques (eigenspace analysis and eigenvalue elasticity analysis) to such nonlinear individual-based infectious disease models, we aim to investigate the effectiveness of linear eigenspace-based approaches for assessing the sensitivity of model behaviors to a parameter for such nonlinear models of infectious disease spread.

First, we apply eigenvalue and eigenvalue elasticity analysis to analyze the evolution of the system behaviors of a nonlinear individual-based viral dynamic model with a small population size as a tool of parameter sensitivity analysis in order to identify parameters that have great impacts on the system, as well as proper time points to perturb these parameters with the purpose of altering the system evolution. Drawing on eigenspace techniques employed in previous studies of model behavior, we find that for nonlinear systems, eigenvalues are effective to understand short-term behaviors, but form a poor tool determining for the long-term impacts of a change on behaviors. This reflects the fact that, for a non-linear system far from equilibrium, eigenvalues of the Jacobian matrix at a particular time point only represent local behavior modes for a short period of time. In addition, we find that for an individual-based model in which each person in the population is driven by similar sets of of equations, the efficiency and insight obtained from eigenspace analysis can be hindered by the repeated occurrence of the same eigenvalue (eigenvalue multiplicity). In eigenvalue elasticity analysis, while changes of parameters based on eigenvalue elasticities could yield significant changes to eigenvalues in a short period of time, such changes may not translate into pronounced changes in state behaviors. In terms of disease control, local changes of eigenmodes are able to alter behaviors in a short-term, especially in the period of the disease outbreak, though such changes may not be sufficient to decrease the prevalence or average infection among the population in the later stages of disease spread, as system behaviors approach stable endemic equilibria. We found that for highly nonlinear systems, a focus on the dominant eigenvalues – or even all eigenvalues – alone may not be sufficient to describe the dynamics of the system even in a short time period, given that the structure of eigenvectors, as well as coefficients, could mediate and moderate the impacts

of such an eigenvalue change on state variables in important ways. This difficulty poses particular challenges for larger systems, because of the large number of state variables and eigenvalues, as well as their associated coefficients and eigenvectors.

The remainder of the paper is arranged as following: Section 2 reviews the past related work on eigenvalue elasticity analysis. Section 3 describes the individual-based viral dynamic models with different population size and their behavior in the state space. Section 4 analyzes an individual-based viral dynamic model with eigenvalue elasticity methods. Finally, in Section 5 we give conclusions and future directions for our study.

2   Related Work of Eigenvalue Elasticity Analysis

The methodology of eigenvalue elasticity analysis was first introduced to the field of system dynamics by N. Forrester in 1982 [4]. Eigenvalues can be regarded as defining different behavior modes, the superposition of which describes the overall behavior of the system. In his dissertation, he proposed the concept of eigenvalue elasticity and used this concept relative to model feedback structure to understand model behaviors. His studies of eigenvalue elasticity indicated that a parameter with higher eigenvalue elasticities is more important than those with lower elasticities to the system. He described the magnitude of 'the loop elasticity' as a measurement of the significance of a feedback loop to a dynamic behavior mode. Because the sum of all link elasticities arriving at one node equals the sum of all link elasticities departing this node, 'link elasticity' was defined as a sum of all loop elasticities passing through a link. With this definition, it is possible to set up a linear system to identify the loop elasticities of the model for each eigenvalue of the system matrix. Forrester applied this methodology in a linear system and a nonlinear system which was linearized for particular time points.

Recent work on loop dominance analysis was contributed by Saleh. In his work, he refined many aspects of eigenvalue analysis, especially in nonlinear models. In [12], he suggested that eigenvalue elasticity analysis is also suited for nonlinear systems by noting how the eigenvalues change as causal link gains change in the linearized model in addition to examining conventional computation of eigenvalues of the Jacobian matrix at particular time points. In his study, eigenvalue elasticity analysis provides a method to identify the dominant structures (e.g., loops) in the model [13].

As an improvement of formal dynamic model analysis tools, Guneralp [6, 5] proposed a ten-

step procedure to measure all modes of the model and to calculate the elasticity values with a normalized method, which overcomes the drawbacks, particularly the computational expenses, of the traditional experimental iterative analysis of models. The methodology is able to track the loop dominance dynamics over time and the influences of feedback loops on a specific variable. This method also made it possible to plot relative loop elasticities over time for visualization of how loop dominance dynamics unfold through simulation [6]. His analysis is useful in understanding the impact of the structural causes underlying oscillations and the other modes of system behavior, as well as potential policy options for prevention and management of an economic system. However, the methodology was shown to be effective only for simple nonlinear systems with a small number of state variables (less than ten), and the influences of evolutions of eigenvectors and coefficients on the system analysis were not discussed.

3 Individual-based Viral Dynamic Models: Descriptions

Most extant dynamic infectious disease models can be classified as either compartmental models or individual-level network models [8]. The dynamics of compartmental models are usually described by ordinary differential equations, an example being the SIR model (Susceptible-Infected-Recovered) [15]. This type of model presents dynamics of infectious disease transmission at an aggregated level, and such models commonly impose assumption of continuous mixing of population within compartments [11]. SIR models and their variants are epidemiological models that compute the theoretical value of population who are infected with an infectious disease in a closed population over time [15]. One of the simplest and earliest examples of SIR models is the Kermack-McKendrick model [7], and many variants of this model exist, with multiple classes of infective and susceptible individuals [10].

While powerful, aggregate infectious disease models pose difficulties in characterizing the detailed impacts of network contact between individuals in the population on the progress of disease spread. This poses a problem, for example, for some sexually transmitted diseases, of which the transmission exhibits distinct complex dynamics in some sub-groups such as a particular ethnic group or a group of sex trade workers [2], and where it is of great value to understand such detailed dynamics for the sake of planning targeted, network-conscious interventions (such as contact tracing regimens, tailored needle exchange programs, etc.). Social network analysis and agent-based modeling of infectious diseases spread can help us identify the significant people in the network
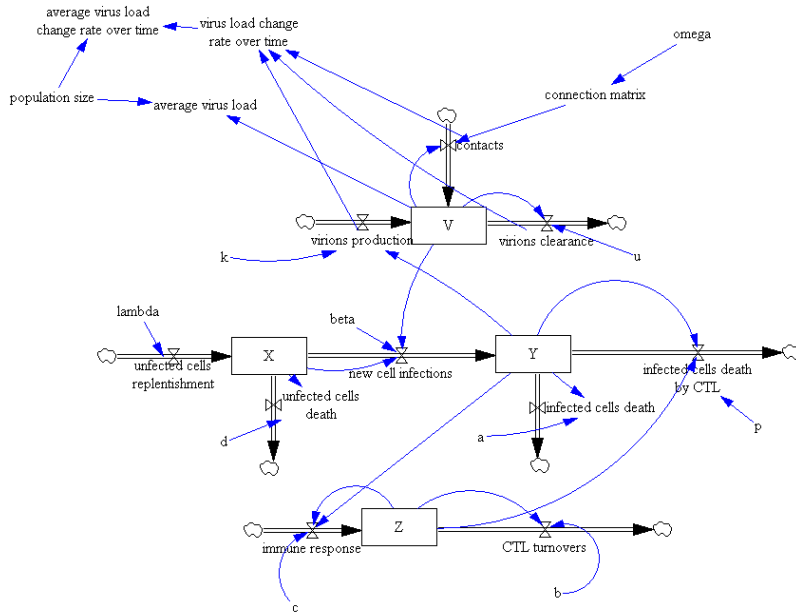
Figure 3.1: The stock-flow diagram of an individual-based viral dynamic model.

to whom public health field nurses or policy makers should pay more attention. However, classic social network analysis mainly emphasizes static network properties and characteristics of nodes in the network, and therefore cannot provide insight into the best time and important factors of each individual to control the spread of infectious diseases. In addition, most agent-based models use discrete rules to describe inner state transitions for each agent in the network, which typically have only coarse representations of individual-level dynamics, such as the dynamics of infection, building of naturally acquired or vaccine introduced immunity, and waning of immunity. Reliance on such discrete transitions within individual-based models can inhibit more detailed understanding of individual dynamics, and – equally importantly – can raise barriers to insight into the location and stability of equilibria.

In the level of individual biological dynamic processes, differential equation based mathematical models of disease dynamics incorporating aspect of immunology and virology have recently begun to provide details of dynamics of infected cells, uninfected cells, virus, and immune responses.

Our base virus dynamic model for an individual contains four state variables: the population size of uninfected cells x, the population size of infected cells y, the number of free virus particles v, and cytotoxic T lymphocytes (CTL) z. The state equations of the model are based on those of [9].

Table 3.1: Parameter settings of an individual-based viral dynamic model.

Parameter	Full Name	Value	Units
β	the rate of uninfected cells to be infected	10^{-5}	1/day·virions
k	the rate of infected cells to produce free virus	3	virions/day·cells
d	the death rate of uninfected cells	0.1	day^{-1}
u	the death rate of free virus	3	day^{-1}
a	the death rate of infected cells	0.5	day^{-1}
λ	the replenishing uninfected cell rate	10^5	cells/day
p	the rate of infected cells to be eliminated by the CTL response	1	1/day·CTLs
c	the production rate of CTL	0.7	1/day·CTLs
b	the death rate of CTL	0.05	day^{-1}

$$\dot{x} = \lambda - dx - \beta xv$$
$$\dot{y} = \beta xv - ay - pyz$$
$$\dot{v} = ky - uv \qquad (3.1)$$
$$\dot{z} = cyz - bz$$

The units for x, y, v, and z are cells, cells, virions, and CTLs, respectively. Explanations and initial settings of parameters are listed in Table 3.1.

Fig. 3.2 describes the early stage of dynamical changes of the state variables of the individual in one person model described by Eq. 3.1. The initial conditions for this one person model are $x(0) = 10^6, y(0) = 0, v(0) = 0.01, z(0) = 1$. Infected by initial viruses, and then by endogenously produced viruses, the number of infected cells, y, increases exponentially at the beginning of the system evolution and at the same time the number of uninfected cells, x decreases. Shortly after the rise of infected cells, y, the viral load, v, begins to increase exponentially because of the release of virions from infected cells. Later, the value of z, representing the number of CTLs, grows, reflecting CTLs proliferation in response to the rise of infected cells. z declines more slowly than y and v so that the individual largely clears the infection and receives some degree of protective immunity. Because the number of infected cells decreases, the immune response begins to decline. As their protective immunity wanes, a 'critical' point is reached at which the rate of the death of infected cells falls below the rate of infection of cells and y begins to increase again. The amount of CTLs does not decline to zero because when it is decreasing infected cells start to increase. Because of the immune memory built up in response to the first infection, the second peak value of y is much

smaller than the first one. We should note here the scale of infected cells, viral loads and CTLs in this figure are relatively small compared with that of uninfected cells because of our default parameter settings. Practically, the values of parameters vary over different types of diseases, and for the purpose of methodology study we did not calibrate the model and parameter settings with real data. The reader can choose to view the state variables and parameters as associated with specific dimensions but arbitrary units.
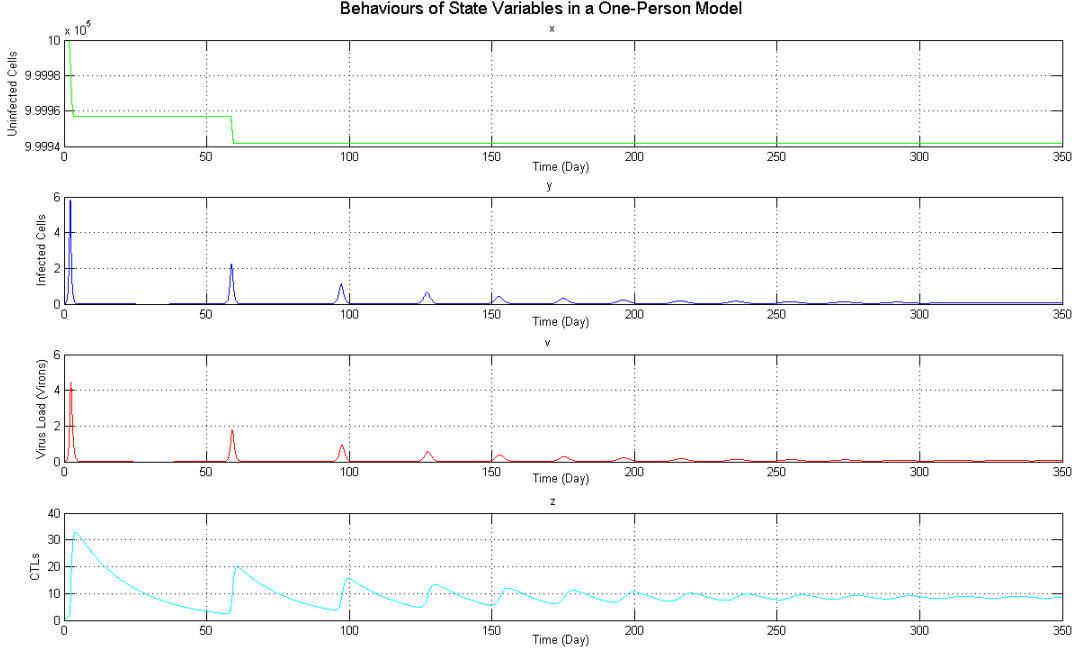
Figure 3.2: Dynamic behaviors of state variables in one-person model.

To understand the implications of individual viral dynamics for infection spread in the population, we follow the multi-individual model depicted in [14], whose state equations are shown as Eq. 3.2, and whose stock and flow structure is shown in Fig. 3.1. In this model (which differs from the previous model only in the 3rd component), an individual interacts with others in form of exchanging free virus v.

$$
\begin{aligned}
\dot{x}_i &= \lambda - dx_i - \beta x_i v_i \\
\dot{y}_i &= \beta x_i v_i - a y_i - p y_i z_i \\
\dot{v}_i &= k y_i - u v_i + \omega \sum_{i \neq j} \sigma_{ij} v_j \\
\dot{z}_i &= c y_i z_i - b z_i
\end{aligned}
\tag{3.2}
$$

Where, $i, j = 1, \cdots, P$ and P is the size of population.

7

σ_{ij} indicates whether the ith individual and the jth individual are connected. This parameter varies for different individuals in the network, and we assume that $\sigma_{ij} = \sigma_{ji}(i \neq j)$ and $\sigma_{ii} = 0$. ω is the connection weight between individuals, with the unit of 1/day.

In such individual-based models, the behaviors of state variables for each individual are influenced not only by values of parameters, but also by network structures and population size.

We call the individual in the above one person model `Person 1` and add another person (`Person 2`), who is free from disease initially (i.e., $x_2 = 10^6, y_2 = 0, v_2 = 0, z_2 = 1$). Connect those two individuals with connection weight (ω) 10^{-6}, yielding the resulting connection matrix:

$$(\sigma_{ij})_{2\times2} = \begin{pmatrix} 0 & 1 \\ 1 & 0 \end{pmatrix}$$

Furthermore, we add the third person connected to `Person 2` with the same weight and initial conditions (to form a line-shape three-person model), the connection matrix becomes:

$$(\sigma_{ij})_{3\times3} = \begin{pmatrix} 0 & 1 & 0 \\ 1 & 0 & 1 \\ 0 & 1 & 0 \end{pmatrix}$$

Behaviors of state variables in the system over time are plotted in Fig. 3.3, where the X-axis is time and Y-axis represents the level of viral loads/uninfected cells/infected cells/CTLs.

4 Eigenvalue and Eigenvector Analysis

In a very short period around a particular point of time, a linearized model with Jacobian matrix can be an excellent approximation to its associated nonlinear model [4]. The following sections describe dynamic behaviors of the individual-based model through eigenvalues and eigenvectors of a linearized individual-based model described at each time point.

For the model described by Eq. 3.2, there are $N = 4P$ states and correspondingly $4P$ eigenvalues of the system's Jacobian matrix. It is difficult to compactly describe all states and eigenvalues clearly for a system with a large population, therefore in this section, we start the study with a model of small populations: the line-shape three-person model, where $P = 3$.
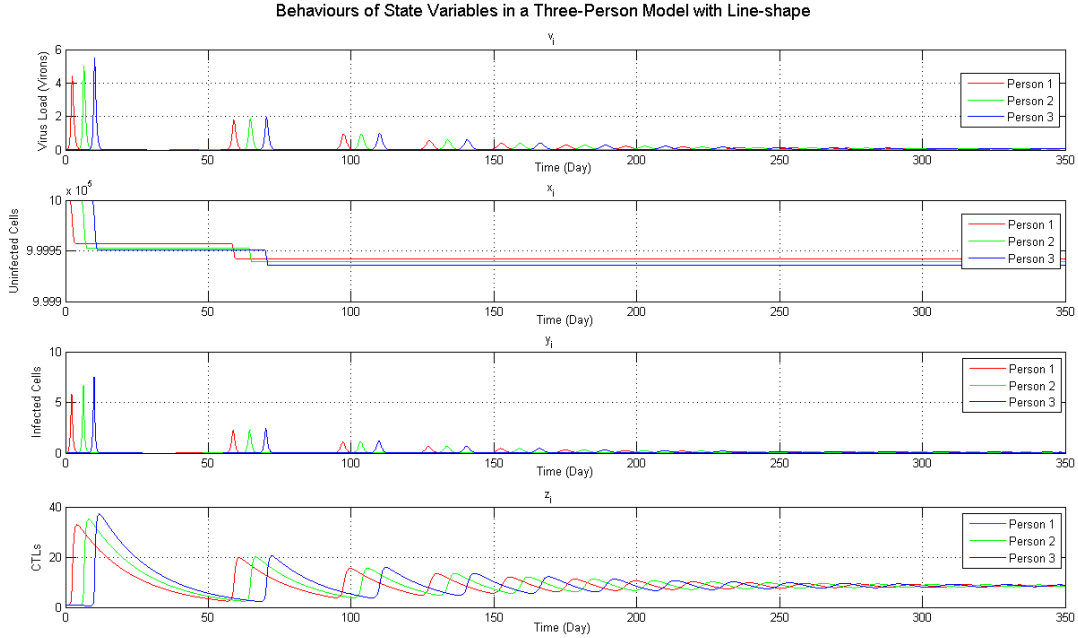
Figure 3.3: Behaviors of state variables for an individual-based model with 3 persons in line-shape.

4.1 Eigenvalue Analysis of an Individual-based Viral Dynamic Model with 3 Persons

4.1.1 Eigenspace Analysis

Approximating the system to be a linear one at regularly spaced time points with the Jacobian matrix, we obtained eigenvalues of the Jacobian matrix over time.[1]

Fig. 4.1 shows all real components of eigenvalues of the Jacobian matrix of the model over time, where the horizontal axis is time and the vertical axis shows the value of real components of eigenvalues. As time increases, the magnitude of oscillation of the eigenvalues becomes quite small, which means the system tends towards an equilibrium, at which the state variables – and hence the eigenvalues – maintain constant values. Because of the relatively large number of eigenvalues in the system, the relationship between the system behaviors and eigenvalues is still not intuitively clear. In the following part of this section, we focus on the dominant eigenvalues[2], i.e., the eigenvalues

---

[1]Usually the linearization of a nonlinear system produces an inhomogeneous linear system, and we show in Section A.1 that such inhomogeneity does not influence the analysis with eigenspace methods.

[2]Definitions of the concepts of dominant eigenvalues, dominant eigenvectors and coefficients can be found in Section A.2

Figure 4.1: The real components of all eigenvalues over time for an individual-based viral dynamic model with 3 persons in line-shape.

with the largest real parts. Fig. 4.2 gives both the real and imaginary parts of the dominant eigenvalues over time for the 3-people model, where the horizonal axis is time axis and the vertical axis presents the value of real and imaginary parts of the eigenvalues.

The largest real parts of the eigenvalues oscillate dramatically before $time = 200$, and its imaginary part is nonzero when the real part falls at the end of each period. Correspondingly, in general, behaviors of the states x_i, y_i, v_i and z_i ($i = 1, 2, 3$) appear with pronounced oscillations during this period of time, as shown in Fig. 3.3. From $time = 200$ to $time = 300$, the magnitude of the oscillation of the imaginary parts are smaller, indicating the damping time for each oscillation is a bit longer than in the previous period. After $time = 300$, both real and imaginary parts of the dominant eigenvalue became increasingly stable. Eventually, the real part of the dominant

10

The Eigenvalue with the Largest Real Part for Three People Virus Dynamics Model
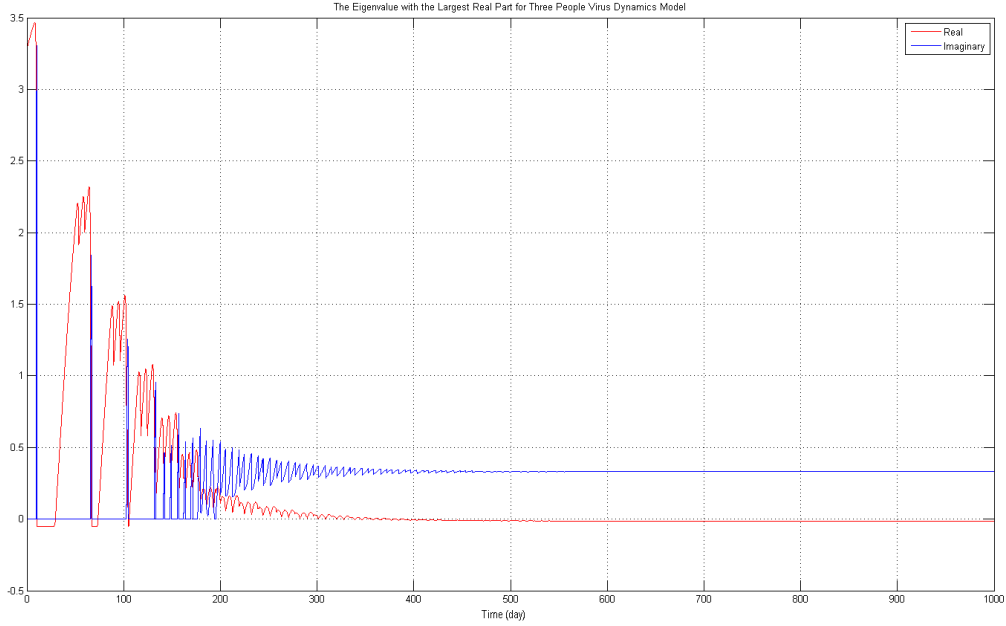
Figure 4.2: The largest real component of eigenvalues and the corresponding imaginary component over time for an individual-based viral dynamic model with 3 persons.

eigenvalue is below zero, and the imaginary part is around 0.35, which means the system decays toward an equilibrium with a almost constant frequency of oscillation, as shown in Fig. 3.3.

Because of the long time frame involved and the pronounced dynamics, the dynamics of behaviors and their corresponding eigenmodes in Fig. 3.3 is not fully clear. The following part of this section therefore focuses a short period of time when the dominant eigenvalues are complex. For example, from $time = 9.54$ to $time = 10.28$, the imaginary part of dominant eigenvalues are nonzero, and the state variables v_2 and y_2 oscillate during this period. Fig. 4.3 gives local views of state variables in this period of time. In this period, x_2 decreases while x_1 and x_3 slowly increase; y_2 increases first and declines later, while y_1 and y_3 are almost zero; v_2 increases while v_1 and v_3 are almost zero; and z_2 begins to increase at later time while z_1 and z_3 are slowly decreasing. Particularly, four phases in this period are listed as: phase I ($time = 10.04$ to $time = 10.09$), phase II ($time = 10.10$ to $time = 10.15$), phase III ($time = 10.16$ to $time = 10.21$), and phase IV ($time = 10.22$ to $time = 10.28$). The dominant eigenvalues of these four phases are: $2.277 \pm 3.263i$, $1.493 \pm 3.307i$, $0.6693 \pm 3.023i$ and $0.00394 \pm 2.524i$. The real parts of the dominant eigenvectors

11

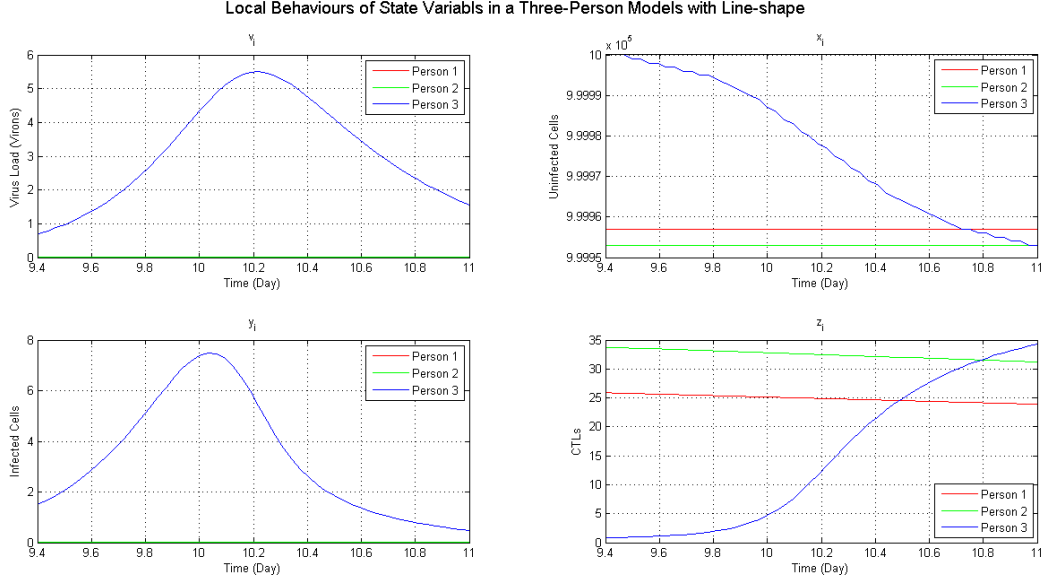Figure 4.3: An early view of behaviors of state variables for an individual-based viral dynamics model with 3 persons, where v_1, v_2, y_1, and y_2 are near zero.

of the four phases are listed respectively in the following:

$$
\begin{array}{c}
x_1 \\
y_1 \\
v_1 \\
z_1 \\
x_2 \\
y_2 \\
v_2 \\
z_2 \\
x_3 \\
y_3 \\
v_3 \\
z_3
\end{array}
\begin{pmatrix}
+2.440 \times 10^{-11} \\
+2.593 \times 10^{-15} \\
+7.709 \times 10^{-15} \\
+1.674 \times 10^{-15} \\
-8.896 \times 10^{-8} \\
+1.235 \times 10^{-8} \\
+4.299 \times 10^{-8} \\
+5.287 \times 10^{-8} \\
-6.184 \times 10^{-1} \\
+3.905 \times 10^{-2} \\
+1.470 \times 10^{-1} \\
+3.740 \times 10^{-1}
\end{pmatrix},
\begin{pmatrix}
-1.398 \times 10^{-11} \\
+3.164 \times 10^{-15} \\
+8.986 \times 10^{-15} \\
-1.811 \times 10^{-15} \\
-9.466 \times 10^{-8} \\
+1.315 \times 10^{-8} \\
+4.428 \times 10^{-8} \\
+5.590 \times 10^{-8} \\
-6.432 \times 10^{-1} \\
-8.102 \times 10^{-2} \\
+1.025 \times 10^{-1} \\
+4.787 \times 10^{-1}
\end{pmatrix},
\begin{pmatrix}
-4.835 \times 10^{-11} \\
+4.143 \times 10^{-15} \\
+1.160 \times 10^{-14} \\
-8.211 \times 10^{-15} \\
-1.099 \times 10^{-7} \\
+1.402 \times 10^{-8} \\
+4.547 \times 10^{-8} \\
+6.517 \times 10^{-8} \\
-6.859 \times 10^{-1} \\
-1.444 \times 10^{-1} \\
+5.278 \times 10^{-1} \\
+5.561 \times 10^{-1}
\end{pmatrix},
\begin{pmatrix}
-6.841 \times 10^{-11} \\
+6.000 \times 10^{-15} \\
+1.607 \times 10^{-14} \\
-1.672 \times 10^{-14} \\
-1.380 \times 10^{-7} \\
+1.412 \times 10^{-8} \\
+4.429 \times 10^{-8} \\
+8.335 \times 10^{-8} \\
-7.298 \times 10^{-1} \\
-1.447 \times 10^{-1} \\
+1.018 \times 10^{-2} \\
+5.889 \times 10^{-1}
\end{pmatrix}
$$

From these eigenvectors, it can be observed that during this period of time, components in the dominant eigenvectors which represent states of `Person 3` (the final 4 components) have larger values than other components, which means in this period, the dominant eigenvalue primarily determines the behavior mode of `Person 3`. In Fig. 3.3, the states of other two persons exhibit little

12

change, and those of `Person 3` alter significantly. Complex eigenvalues here indicate oscillations of y_3 and v_3. In fact, x_3 and z_3 also oscillate before and after this period respectively. Because new virions are mainly produced by infected cells, the oscillation of v_3 occurs a bit later than that of y_3; meanwhile z_3 begins to grow a bit later than y_3 because CTL proliferates in response to the growth of infected cells. In phase I and II, components of y_3 in the dominant eigenvector are relatively smaller, and its change rate $\dot{y}_3$ is smaller than the change rates of other three states, as shown in Fig. 4.4. In all of these four phases, components representing x_3 in the dominant eigenvectors have relatively large absolute values, and its changing rate $\dot{x}_3$ is also very large.
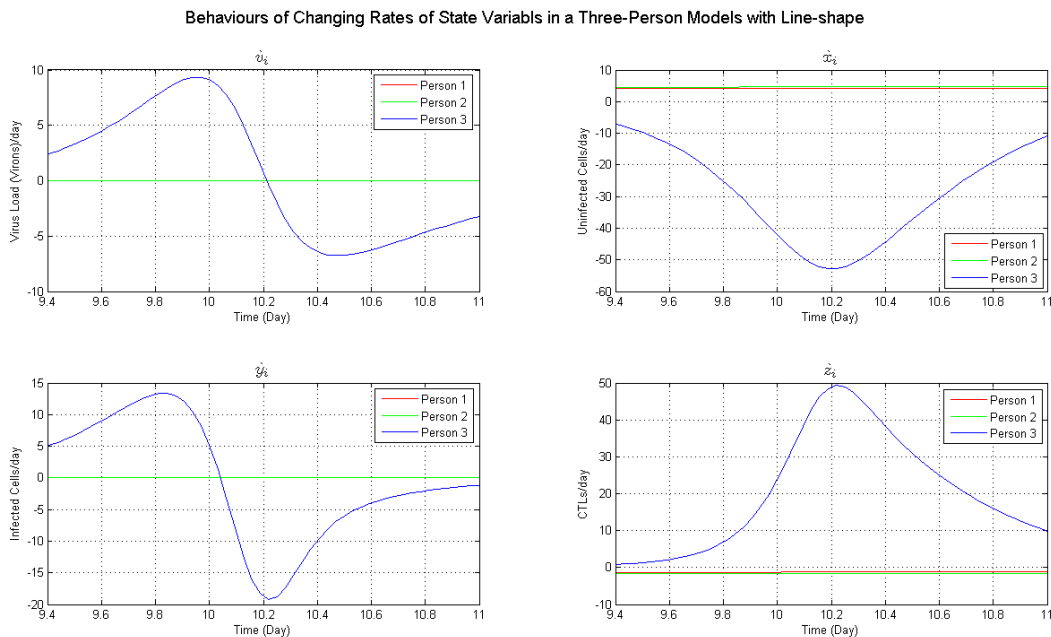
Figure 4.4: An early view of $\dot{v}_i, \dot{x}_i, \dot{y}_i, \dot{z}_i$ $i = 1, 2, 3$ for an individual-based viral dynamic model with 3 persons in line-shape.

4.1.2 Multiplicity of Eigenvalues

If we add another person, `Person 4` connected with `Person 2` in the three-person "line-shaped" model, who has the same connections and initial values as `Person 3` and re-analyze the model, from symmetry considerations we would expect that the final 4 entries of the eigenvectors (representing `Person 4`) and the second last 4 entries of eigenvectors (representing `Person 3`) to be identical. However, for some eigenvectors (usually the last 6 eigenvectors) entries for `Person 3` and `Person 4` are not identical. One reason for that is eigenvalue multiplicity.

13

An eigenvalue of the square matrix A is of multiplicity of K if it is a K-fold root of the characteristic equation $|A - \lambda I| = 0$. If an eigenvalue has K linearly independent associated eigenvectors, this eigenvalue of multiplicity K is complete. However, not all multiple eigenvalues are complete, and an incomplete eigenvalue of multiplicity of $K > 1$ can be termed defective [3]. A matrix with any defective eigenvalue is called a defective matrix. The computation of eigenvalue solutions for linear (or linearized) differential equations with defective eigenvalues is very complicated, and its eigenspace is also hard to analyze.

In our study, at $time = 0.5$ the last 4 eigenvectors share the same eigenvalue -0.1, associated with die-off of uninfected cells, which comes from the constant entry of the Jacobian matrix, and the second last four eigenvalues are -0.05, associated with die-off of infected cells. These two eigenvalues are of multiplicity of 4. At $time = 0.5$ the rank of the matrix of eigenvectors is 16, and the matrix is of full rank[3]. Thus eigenvectors at this time point are linearly independent. We checked eigenvectors of the Jacobian matrix at several time points when the multiplicity of eigenvalues occurs, and we found that all these eigenvectors are linearly independent. Hereby we assume (though do not prove) that in the model examined here, when there are multiple eigenvalues, they are complete and their corresponding eigenvectors are linearly independent. Thus the expansion of state variables around a point $\mathbf{x}_0$ at time t_0 could be presented as the following:

$$\mathbf{x}(t) = \sum_{i=1}^{16} c_i \mathbf{r}_i e^{-\lambda_i(t-t_0)} + \mathbf{b} \tag{4.1}$$

Where $\mathbf{x}$ is the vector of state variables, $\mathbf{r}_i$ is the ith eigenvector of the Jacobian matrix of the system, and $\mathbf{b}$ is the constant term. As we indicated in Section A.1, the constant term does not affect the analysis of eigenmodes and behavior patterns, and thus we neglect this constant term in following discussions. For this model, the last four eigenvalues are -0.1 and the second last four eigenvalues are -0.05. Therefore, we could rewrite the expansion of λs in Eq. 4.1 into the eigenmodes as:

$$\mathbf{x}(t) = \sum_{i=1}^{8} c_i \mathbf{r}_i e^{-\lambda_i(t-t_0)} + (\sum_{i=9}^{12} c_i \mathbf{r}_i) e^{-0.05(t-t_0)} + (\sum_{i=13}^{16} c_i \mathbf{r}_i) e^{-0.1(t-t_0)} \tag{4.2}$$

The last two weighted eigenvectors $\sum_{i=9}^{12} c_i \mathbf{r}_i$ and $\sum_{i=13}^{16} c_i \mathbf{r}_i$ can be calculated yielding the following:

$$\sum_{i=13}^{16} c_i \mathbf{r}_i = [\ldots, -1.49 \times 10^{-3}, -1.24 \times 10^{-17}, 2.30 \times 10^{-16}, 1.69 \times 10^{-16},$$

---

[3]This matrix of eigenvectors is listed in Section Appendix C.

$$-1.49 \times 10^{-03}, -1.24 \times 10^{-17}, 2.30 \times 10^{-16}, 1.69 \times 10^{-16}]^T$$

$$\sum_{i=9}^{12} c_i \mathbf{r}_i = [\dots, 5.89 \times 10^{-9}, 9.86 \times 10^{-11}, -1.44 \times 10^{-9}, -4.88 \times 10^{-2},$$

$$5.89 \times 10^{-9}, 9.86 \times 10^{-11}, -1.44 \times 10^{-9}, -4.88 \times 10^{-2}]^T$$

From the above, we can see that sum of eigenvector entries representing for `Person 3` and `Person 4` are identical. This suggests that for an individual-based model, if several individuals share the same parameters, connections, and initial conditions we could group them together and regard them as a single individual with multiple links. In addition, because the individuals in the network share similar equations, and some of them share the same parameters and initial conditions, the multiplicity of eigenvalues occurs frequently for the individual-based model, as shown in Fig. 4.1. This might be a significant limitations of eigenvalue analysis for individual-based models, and merits further investigation.

4.2 Eigenvalue Elasticity Analysis

As defined in [4], the ***eigenvalue elasticity with respect to a parameter*** is defined as the partial derivative of the eigenvalue with respect to that parameter normalized for the size of the parameter and the size of the eigenvalue. Equivalently, assuming a non-zero value of the parameter (an important limitation), the elasticity of eigenvalue could also be described as the product of the eigenvalue sensitivity and the ratio of the eigenvalue and parameter. Thus the eigenvalue elasticity of λ_i, with respect to a parameter p_j is as Eq. 4.3.

$$\epsilon_i(p_j) = \lim_{\Delta p_j \to 0} \frac{\frac{\Delta \lambda_i}{\lambda_i}}{\frac{\Delta p_j}{p_j}} = \frac{\frac{\partial \lambda_i}{\lambda_i}}{\frac{\partial p_j}{p_j}} = \frac{\partial \lambda_i}{\partial p_j} \cdot \frac{p_j}{\lambda_i} \tag{4.3}$$

In this definition, since $[\partial \lambda_i] = [\lambda_i]$ and $[\partial p_j] = [p_j]$ ($[\bullet]$ denoting the unit of $\bullet$), eigenvalue elasticity is dimensionless, enabling us to compare elasticities of the eigenvalue with respect to different parameters. Therefore, if an eigenvalue elasticity with respect to one parameter is larger than for others, it is interpreted as meaning that behavior mode is more sensitive to a certain proportional change in that parameter than to similar proportional changes in other parameters. A similar comparison of elasticities is also possible between different time points.

There are ten parameters for the individual-based viral dynamics model; however, although eigenvalue elasticities with respect to parameters can be analyzed mathematically, some of these parameters are difficult to alter biologically, for example, β (`the rate at which uninfected cells`

are infected). In this section, we focus on the parameter c (`the production rate of CTL`) and ω (`the connection weight`) and the eigenvalue elasticity with respect to them, because practically c might be changed by behavior changes (e.g. exercise, smoking cessation, improved nutrition) or medical treatments (e.g. prevention of progress of kidney disease), and ω can be perturbed by social policies, such as policies to reduce risk-taking behaviors or to enhance hygiene or encourage reduced mixing.

Because we have 12 eigenvalues for this individual-based viral dynamics model, it is natural to find the eigenvalue elasticities with the largest real parts and to try to perturb this parameter at the time point when the first peak in eigenvalue elasticity appears. ("Perturb a parameter" here means to change the value of a parameter from a time point to the end of simulation time.)

Fig. 4.5 plots the largest real parts of eigenvalue elasticity with respect to ω, and its corresponding imaginary parts. In this study, the largest eigenvalue elasticity in this study means the maximum value of elasticity over all eigenvalues. From these two figures, it can be observed that the first peak of the real parts of the eigenvalue elasticity appears from $time = 0$ to $time = 0.03$ with the value of 1.86×10^{-7}, the second significant peak appears from $time = 139.10$ to $time = 139.15$ with the value of 1.02×10^{-7}, and the elasticity arrives at the highest value of 4.53×10^{-7} when $time = 934.04$. The imaginary part of the elasticity at the first and the second peak is zero, and is 1.52×10^{-6} at the time of the third peak.

As mentioned earlier, a parameter with higher eigenvalue elasticities is more important than those with lower elasticities to the system. As a policy lever, the perturbation of this parameter might be more effective than that of other parameters. However, we also want to know proper times to change the parameter. In our study of infectious disease, it is generally desirable to intervene earlier because we want to reduce the number of infected people and delay the spread of diseases. Here, although the eigenvalue elasticity with respect to ω arrives at the highest peak at $time = 934.04$, it is nearly meaningless to perform a policy at this time in practice because the system approaches to an equilibrium after $time = 500$ and any change then will not influence the system too much. (The constraints of global structure on the long-term impact of local perturbations is a topic to which we return later.) Therefore, we perturb ω at $time = 0.03$ (when the largest eigenvalue elasticity is relatively high in comparison to other points, namely 1.86×10^{-7}) and $time = 139.1$ (when the largest eigenvalue elasticity is 1.02×10^{-7}). A simulation of a perturbation of ω at $time = 10$ (when the largest elasticity is comparatively small at -3.58×10^{-12}) is performed
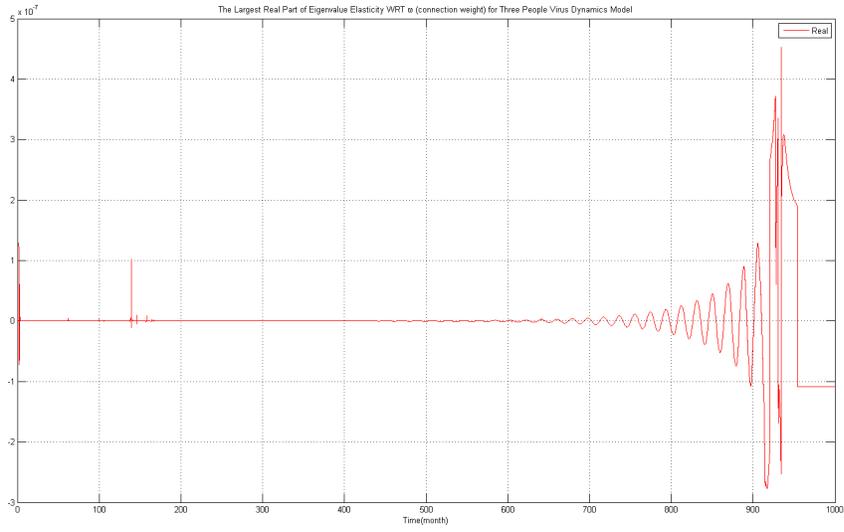
(a) Real Parts
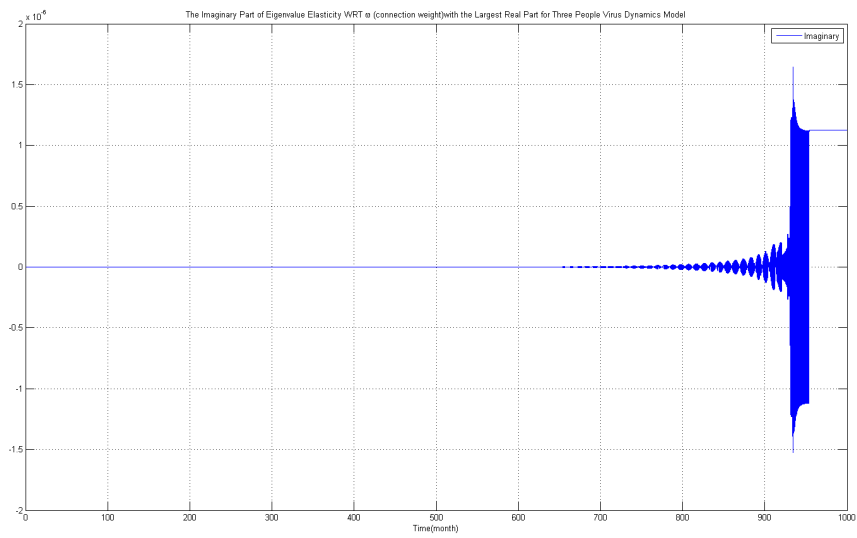
(b) Imaginary Parts

Figure 4.5: The largest real part of eigenvalue elasticity with respect to ω (`the connection weight`) for an individual-based viral dynamic model with 3 persons and the corresponding imaginary parts.

as a control. We decrease ω to be 90% of the original value of 10^{-6} for the perturbation[4].

We expect that the perturbation at $time = 0.03$ when the elasticity is relatively high could yield more significant changes of the system behaviors than the perturbations at other two time points in the simulations. However, the change of behavior is quite small and the difference between perturbations at different time points are difficult to observe (as shown in Fig. B.1) because of small changes of ω and small values of the elasticities. Therefore, we exert a bigger alteration on ω, and change it to be 10% of its original value. Shortly after the perturbations of ω at $time = 0.03$, $time = 10$, and $time = 139.1$, the average of v across the population does not change at all. In a longer period of time, the perturbation at $time = 0.03$ and the control (at $time = 10$) delay the oscillations of the mean value of v over the population. However, the perturbation at $time = 139.1$, when a comparatively large eigenvalue elasticity appears, does not change the behavior of the average v at all.

The above analysis suggests that a small change of the parameter ω does not always produce visible changes of the system behaviors. Based on Eq. 4.3, we have

$$\Delta \lambda_i \approx \epsilon_i(p_j) \frac{\Delta p_j}{p_j} \lambda_i \tag{4.4}$$

With a given change of p_j, the value of $\Delta p_j / p_j$ is fixed, and the change of λ_i is determined by both the elasticity and the eigenvalue itself. From Table 4.1, it can be observed that at $time = 139.1$, the eigenvalue corresponding to the largest elasticity is much smaller than the dominant eigenvalue. In contrast, for the low-elasticity control experiment at $time = 10$, the eigenvalue corresponding to the largest elasticity is with the same order of magnitude of the dominant eigenvalue; and at $time = 0.03$ the eigenvalue with the largest elasticity is the dominant eigenvalue at that time. Therefore, we conjecture that the perturbation at $time = 0.03$ alters the system behavior most significantly, because the perturbation of the parameter affects the dominant eigenvalue.

From the above analysis, we know that a small change of ω does not result in a significant alteration of the system behavior even in the short-term because the elasticity of the eigenvalue with respect to ω is of the order of magnitude of 10^{-7} or less in the early time period (before $time = 500$). Because the eigenvalue elasticity is dimensionless, we can assume that the changes of a parameter with larger elasticities could produce more pronounced changes of the system behaviors. Therefore we now consider the parameter with the largest elasticity. Fig. 4.6 illustrates the real and imaginary parts of the largest eigenvalue elasticity with respect to c (the production rate

---

[4]The simulations with perturbations of a parameter in this section can be found in Section Appendix B

Table 4.1: The dominant eigenvalues and eigenvalues with the largest elasticity at different times for an individual-based viral dynamic model with 3 persons.

Time (Day)	Eigenvalue with the Largest Elasticity	Dominant Eigenvalue	The Largest Eigenvalue Elasticity
0.03	3.278	3.278	1.86×10^{-7}
10.0	-1.744	2.814	-3.58×10^{-12}
139.1	2.738×10^{-3}	6.908×10^{-1}	1.02×10^{-7}

of CTL) respectively. The maximum elasticity of the eigenvalues with respect to c has much larger value than that with respect to ω. The first significant peak of the eigenvalue elasticity with respect to c appears from $time = 94.85$ to $time = 94.9$ with the value of -225.9, and the most significant peak of the elasticity appears from $time = 158.72$ to $time = 158.78$ with the value of -2264. The elasticity also arrives at another peak from $time = 165.97$ to $time = 166.03$ with the value of -747.34.

We perturb c to change it to be 110% of the original value 0.7 at $time = 94.85$ and $time = 158.72$. With a 10% increment of c, the mean value of v in the population at the endemic equilibrium in Eq. 4.5 becomes 0.06493509, decreased by 9.1% from the original value. Such perturbation changes the behavior of the average v in the population in the long run (see Section B.2).

Similar to the perturbation of ω, we also add an experiment to perturb c at $time = 10$ as a control when the elasticity is low ($0.768 \pm 0.362i$). The trajectory of the average v has been changed by the perturbations: The value of the average v across the population becomes smaller in a short period of time after perturbations of c at these time points than the original values, which indicates such policy causes the mean viral loads in the population to decline. In addition, the short-term proportional changes of the average v brought by the perturbation at $time = 158.72$ (when the elasticity is high) is a bit more significant than that from the perturbation at $time = 94.85$. The eigenvalue corresponding to the largest elasticity at $time = 158.72$ is the dominant eigenvalue (3.360×10^{-1}) at that time, while the eigenvalue associated with the largest elasticity at $time = 94.85$ is -3.208×10^{-4}. The coefficients of those two eigenvalues are on the order of magnitude of 10^{-1} at that time when the largest and the smallest order of magnitude of other coefficients are 10^1 and 10^{-5}. According to Eq. 4.4, the change of the behavior mode from the perturbation of c at $time = 158.72$ is a bit more significant than that at $time = 94.85$.

However, similar to the perturbation of ω, as a control experiment the perturbation of c at $time = 10$ alters the system behavior greatly in a short period of time after the perturbation. In fact,
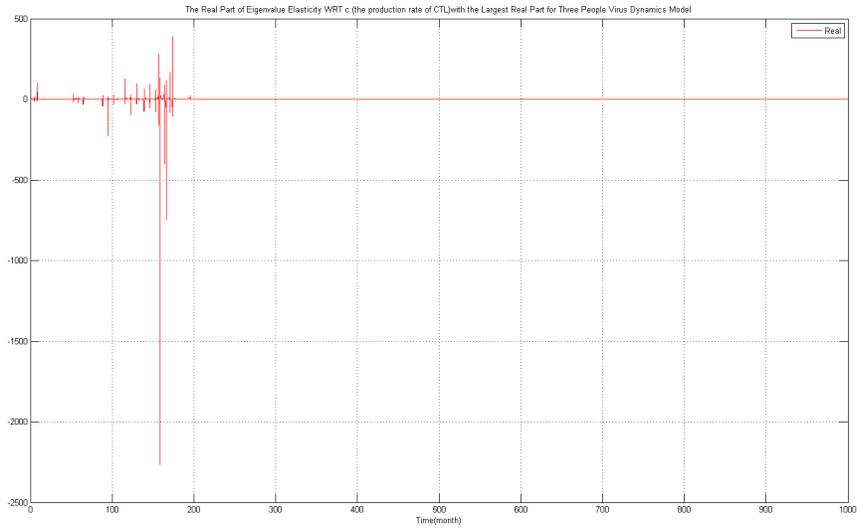
(a) Real Parts
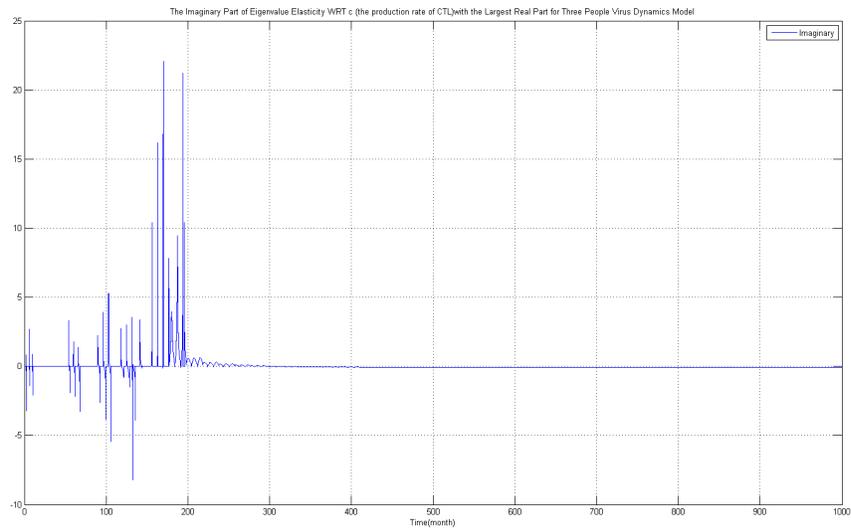
(b) Imaginary Parts

Figure 4.6: The largest real part of eigenvalue elasticity with respect to c (`the production rate of` CTL) for an individual-based viral dynamic model with 3 persons and the corresponding imaginary parts.

the eigenvalue of the largest elasticity is the dominant eigenvalue at that time $(2.814 \pm 2.989i)$. In addition, the coefficient of this eigenvalue is 33.72, the largest coefficient at that time, which means the eigenvector of this eigenvalue must be an eigenvector which dominates the system significantly. Therefore, a small change of the eigenvalue from the perturbation of c can generate distinct changes of the behavior.

We demonstrated above the shortcomings of only paying attention to eigenvalue elasticity in selecting points of intervention. Specifically, this approach fails to take into account the fact that some high elasticities are associated with smaller eigenvalues, and thus are not indicative of a high leverage point. On the basis of this shortcoming, it might reasonably be suggested that, in examining eigenvalue elasticity analysis for time t, one should confine one's attention to the eigenvalue elasticity with respect to the dominant eigenvalue at time t. While there is insufficient space to present the associated experiments here, we note that confining attention purely to elasticity with respect to the dominant eigenvalue also yields poor results. There are three major shortcomings to this approach. First, changes to the "dominant eigenvalue" are often not all that influential to quantities of interest, due to the fact that coefficients associated with this eigenvalue when decomposing the state change vector in the basis of eigenvectors may be very small. While such coefficients for a dominant eigenvector will grow over time, they often will not grow very large over the small period time that this eigenvalue remains dominant. Secondly, because of the structure of the associated eigenvector (small entries associated with relevant state variables), changes to this eigenvalue may not make appreciable difference in modifying global quantities of concern (here, for example, the population-wide mean virus levels). Thirdly, confining attention purely to the dominant eigenvalue overlooks the fact that many other eigenvalues are often of close (or, in the frequent case of complex conjugates, exactly equal) magnitude. Changing these other eigenvalues can have equal or greater impact than changes to the dominant eigenvalue. As a result of these three considerations, while guiding intervention points using only information on elasticity with respect to the dominant eigenvalue alone is attractive from the standpoint of simplicity, it will often overlook high-leverage points of intervention.

Because eigenvalue elasticities at a particular time point are computed with the Jacobian matrix at that time, the largest elasticity can only predict local proportional changes of eigenvalues. Eigenvectors, as well as coefficients, can also jointly determine the short-term evolution of the system – in the presence of a large coefficient or a much larger component, the short-term impact of a given change to a state variable resulting from the perturbation of a parameter with quite modest

elasticity could exceed the impact of a corresponding perturbation to parameter with high elasticity, but whose coefficients and/or eigenvector coefficients are small. For the same reason (and as we found in our experiments), the "dominant eigenvalue" is often not all that influential to quantities of interest and the elasticity of the "dominant eigenvalue" at time t does not necessarily mean the system behavior mode is sensitive to changes of a parameter, due to multiplicities, coefficients and eigenvectors.

As a second independent and equally important critical issue, high eigenvalue elasticities are not necessarily indications of global results of the perturbation of the parameters. We derived the fixed points of the system by setting the derivatives of the state variables to zero, and solving for values of state variables, and obtained symbolic expressions for the endemic equilibrium [9, 14] of the system. At the endemic equilibrium, the average value of v in the population for three-person line-shaped model is [16]

$$\bar{v} = \frac{bk\,(3\,u + 4\,\omega)}{3\,(u^2 - 2\,\omega^2)\,c} \tag{4.5}$$

With the default values of parameters, the population mean value of v at the endemic equilibrium is 0.07142860. From the above formula, in our early experiments when ω is decreased to be 10% of the default value, the population mean value of v at the endemic equilibrium becomes 0.07142857. The difference between the original value and the shifted value is only of the order of magnitude of 10^{-6}. Therefore, because of the equilibrium structure the perturbation of ω by a small amount cannot significantly decrease the mean viral load across the population in the long-term, but could locally alter the trajectory of the average v in the population, and especially at the time points when the elasticity is high and when the eigenvalue with the large elasticity is of magnitude close to the dominant eigenvalue.

Therefore, while high-elasticity perturbations may significantly affect the short-term behavior of trajectories, if those trajectories converge on an endemic equilibrium that remains unchanged, the long-term effect will be minimal. By contrast, a change to a parameter with a small elasticity but which significantly shifts the endemic equilibrium could have very large long-term impact on system state variables.

4.3   Discussion

Unlike the dynamic models discussed in early studies of eigenvalue elasticity, the individual-based viral dynamic model exhibits complexity due to relatively large number of state variables and network connections. Even for the model of three people it is hard to describe the system

behaviors with eigenvalues alone; evolving eigenvectors and coefficients also play an important role in determining the behavior patterns. Repeated eigenvalues of the Jacobian matrix for an individual-based model occur more frequently than for models with a small number of states. All of these difficulties hamper the efficiency of the application of eigenvalue analysis for individual-based models of infectious disease spread.

Because the eigenvalue elasticity is dimensionless, we could compare it with respect to different parameters. In our analysis of the individual-based model, the eigenvalue elasticity with respect to c is much higher than that with respect to ω (by the order of the magnitude 10^8). When both of these two parameters are changed with the same proportion, the changes after perturbations of c are more distinct than after the perturbations of ω. The perturbations of a parameter based on eigenvalue elasticity analysis is also determined by the elasticities, the eigenvalues and their coefficients. For example, an eigenvalue with a small value may have a large elasticity with respect to a parameter, and in such a case, because the eigenvalue does not determine the major behavior of the system, changing the value of the parameter may not result in notable alterations of the system behavior. In addition, the perturbation of a parameter with a large eigenvalue and a large elasticity at a particular point might also have a very limited impact on the system because the coefficient may have a small value. Consequently, the perturbation of a parameter with a high elasticity cannot be guaranteed to yield a significant change of the system behavior over time, even in the short-term. Furthermore, if we analyze a more complex model consisting of 30 or 100 or even one thousand people, the very large number of eigenvalues, parameters, and associated quantities inhibit analysis, and eigenvalue elasticity analysis can likely not provide comprehensive insights. To sum up, the use of eigenvalue elasticity analysis to identify policy levers is not as powerful for a complicated infectious disease model as it can be for simple models.

5   Conclusion

In this paper, we applied local analysis tools, such as eigenvalue and eigenvalue elasticity analysis, to individual-based viral dynamic models and the short-term influences of parameters in a short period of time, especially during a disease outbreak.

Even for such the model with a small population size, eigenvalue analysis is less effective than for the simple models studied in early papers of eigenvalue elasticity, and perturbations of a parameter based on high eigenvalue elasticities could not reliably change state behaviors locally. The first

reason for the challenge is the large number of eigenvalues and eigenvalue multiplicity. Similar mathematical equations and parameter values for each individual make some of the eigenvalues of the Jacobian matrix identical, and it is in general difficult to determine the number of dominant eigenvalues. Secondly, the eigenvalue with high elasticity may not be a dominant eigenvalue or may have a small value for its coefficient which indicates that the corresponding eigenvector is not the major direction of the system evolution. The perturbation of a parameter based on this elasticity thus might not alter the system behavior significantly. Because of the large number of eigenvalues, coefficients and eigenvalue elasticities, it is difficult to understand even the short-term behavior of a large system and to predict the impacts of parameters on the system using the analysis of eigenvalue and their elasticities. Thirdly, the perturbation of a parameter based on the eigenvalue elasticity does not directly work on the state variables, but on the eigenvalues. Although the changes of state variables are small shortly after the perturbation, persistent changes exert their influences in a relatively long run. In terms of the disease control, especially during the outbreak of the disease, such long term effects are not as we expected. All of these difficulties make the eigenspace based methods more complex to analyze nonlinear dynamical systems with a large number of states.

Because eigenvalue elasticity is dimensionless, the method makes it possible for us to compare the importance of parameters for a model, that is capable to help policy makers to find out crucial factors for disease control in a short period of time, especially during the outbreak of an infectious disease. However, the duration of such importance may be brief. An important parameter during the outbreak of a disease could have no influence or unfavorable influence in the long run.

Therefore, we could say that for individual-based viral dynamic models, where the attention is on immediate disease control during a short time period around a disease outbreak, local analysis methods (eigenvalues, eigenvalue elasticity) can be effective to indicate the behavior patterns, the importance of parameters, and the time to change parameters, so that policy makers are able to decrease the prevalence or the severity of the disease in some degree. However, such methodology is effective only over a short period of time. For long term control of the infectious disease spread, other tools should be taken into consideration. One intuitive method involving the problem of eigenvalue complexity could be trying to get rid of the complexity brought by the large number of eigenvalues and eigenvalue multiplicity and developing analysis tools to directly show the impacts of parameters in the state space rather than in the eigenspace. Another aspect is the study of long-term effects of parameter changes on the system behaviors. A particularly attractive, general applicable and powerful way is the closed-form analysis of equilibria. Such equilibria analysis can

take strong advantage of the continuous mathematical structure of system dynamics models to identify the position and stability of equilibria, and drawn on tools such as Routh-Hurwitz criteria to identify the robustness of such stability under parameter perturbation. In this case, policy makers can gain insight as to how to decrease the severity of the infectious disease for a long term benefit, and whether their policies or external factors risks rendering the stable disease free equilibrium unstable so that the pathogen is at risk of triggering additional outbreaks.

By contrast, there are significant hurdles to performing such equilibrium analysis for individual-based models where individual behavior is characterized discretely, and especially where that behavior is not specified in a mathematically transparent fashion – both common characteristics of many traditional agent-based models of infectious disease spread. We believe that the potential for performing such symbolic equilibrium analysis is a considerable advantage of individual-based models represented in the state equation formulation used here. Until these global techniques and similar analytic methods are further adopted and until variants on eigenspace techniques are refined, system dynamicists will continue to rely largely on performing simulation-based sensitivity analysis to gain insights into the short-term and long-term leverage offered by distinct policy levers in infectious disease models.

References

[1] R. M. Anderson and R. M. May. *Infectious Diseases of Humans: Dynamics and Control.* Oxford University Press, 1991.

[2] P. Bearman, J. Moody, and K. Stovel. Chains of affection: The structure of adolescent romantic and sexual networks. *American Journal of Sociology*, 110(1), 2004.

[3] C. H. Edwards and D. E. Penney. *Differential Equations and Boundary Value Problems: Computing and Modeling.* Pearson Education, 3rd edition, 2004.

[4] N. Forrester. *A Dynamic Synthesis of Basic Macroeconomic Theory: Implacations for Stabilization and Policy Analysis.* PhD thesis, MIT, Cambridge, MA, 1982.

[5] B. Guneralp. Progress in Eigenvalue Elasticity Analysis as a Coherent Loop Dominance Analysis Tool. In *Proc. The 23rd International Conference of the System Dynamics Society*, Boston, MA, July 2005.

[6] B. Guneralp. *Exploring Structure-Behavior Relations in Nonlinear Dynamic Feedback Models.* PhD thesis, University of Illinois at Urbana-Champaign, 2006.

[7] W. O. Kermack and A. G. McKendrick. A Contribution to the Mathematical Theory of Epidemics. In *Proceedings of The Royal Society of London*, volume 115 of *A*, pages 700–721, 1927.

[8] J. Koopman. Modeling Infection Transmission. *Annual Review of Public Health*, 25:303–326, 2004.

[9] M. A. Nowak and R. M. May. *Virus Dynamics: Mathematical Principles of Immunology and Virology*. Oxford University Press, 2000.

[10] N. Osgood. The Impact of Healthcare Delays on Infectious Disease Spread: A Simple Model. Presentation for the Saskatoon Chapter of the Canadian Operational Research Society, April 2008.

[11] D. Powell, J. Fiar, R. L. L. Moore, and D. Thompson. Sensitivity Analysis of an Infectious Disease Model. In *Proceedings of the 23rd International Conference of the System Dynamics Society*, Boston, MA, July 2005.

[12] M. Saleh. *The Characterization of Model Behavior and its Causal Foundation*. PhD thesis, University of Bergen, Bergen, Norway, 2002.

[13] M. Saleh, P. Davidsen, and K. Bayoumi. A Comprehensive Eigenvalue Analysis of System Dynamics Models. In *Proc. The 23rd International Conference of the System Dynamics Society*, Boston, MA, July 2005.

[14] D. Vickers and N. Osgood. A Unified Framework of Immunological and Epidemiological Dynamics for the Spread of Viral Infections in a Simple Network-based Population. *Theoretical Biology and Medical Modelling*, 4(49), 2007.

[15] E. W. Weisstein. SIR Model. MathWorld-A Wolfram Web Resource http://mathworld.wolfram.com/SIRModel.html, 2008.

[16] Q. Zhang and N. Osgood. Stability Analysis of one Type of Individual-based Viral Dynamic Models. In preparation.

Appendix A Mathematical Foundations of Eigenspace Analysis

Many past studies treated dynamical systems as homogeneous systems without explanations. However, in most cases there are significant constant terms for a linearized dynamical system. In addition to the fundamental eigenspace analysis for dynamical systems described in [4, 5], we show that an inhomogeneous system can be transformed to a homogeneous system in terms of eigenspace analysis in detail in the following section, and define some key concepts for our analysis.

A.1 From an Inhomogeneous System to a Homogeneous System

For a nonlinear system, a linearized model at a particular time point t_0 can be derived by a Taylor expansion around t_0:

$$\dot{\mathbf{x}}|_{t_0} = f(\mathbf{x}_{t_0}) + J_{\mathbf{x}_{t_0}} \cdot (\mathbf{x} - \mathbf{x}_{t_0}) + H.O.T. \tag{A.1}$$

Where, $J_{ij} = \partial \dot{x}_i / \partial x_j$ is the entry in the ith row and jth column of the Jacobian matrix of the system at the time point t_0. By omitting the higher order terms, Eq. A.1 can be approximated as an inhomogeneous system:

$$\dot{\mathbf{x}} = J_{\mathbf{x}_{t_0}} \mathbf{x} + \mathbf{b} \tag{A.2}$$

For simplicity of expression, we denote $J_{\mathbf{x}_{t_0}}$ as J, and $\mathbf{b} = -J\mathbf{x}_{t_0} + f(\mathbf{x}_{t_0})$ is a constant vector at time t_0.

With differentiation with t in both sides of Eq. A.2, we obtain

$$\ddot{\mathbf{x}} = J\dot{\mathbf{x}} \tag{A.3}$$

Suppose λ_i is one eigenvalue of J, and $\mathbf{r}_i$ is its corresponding (right) eigenvector ($i = 1 \ldots N$). In eigenspace, $\dot{\mathbf{x}}$ can be expressed as a linear combination of the right eigenvectors [5], i.e.,

$$\dot{\mathbf{x}} = \sum_{i=1}^{N} c_i \mathbf{r}_i \tag{A.4}$$

where c_i is the coefficient of the linear combination for the eigenvector $\mathbf{r}_i$. Differentiating Eq. A.4 on both sides, we obtain

$$\ddot{\mathbf{x}} = \sum_{i=1}^{N} \dot{c}_i \mathbf{r}_i \tag{A.5}$$

Equating the righthand sides for $\ddot{\mathbf{x}}$ given by Eq. A.3 and Eq. A.5, and using the definition of $\dot{\mathbf{x}}$ in Eq. A.4, we have

$$J \sum_{i=1}^{N} c_i \mathbf{r}_i = \sum_{i=1}^{N} \dot{c}_i \mathbf{r}_i$$

Because $\mathbf{r}_i$ are the eigenvectors of J, and $J\mathbf{r}_i = \lambda_i \mathbf{r}_i$ $\therefore$

$$\sum_{i=1}^{N} c_i \lambda_i \mathbf{r}_i = \sum_{i=1}^{N} \dot{c}_i \mathbf{r}_i$$

$\therefore$

$$\dot{c}_i = \lambda_i c_i \qquad (i = 1 \cdots N)$$

$\therefore$

$$c_i = c_i(t_0) e^{\lambda_i(t-t_0)} \qquad (i = 1 \cdots N) \tag{A.6}$$

With Eq. A.4 and Eq. A.6, we have

$$\dot{\mathbf{x}} = \sum_{i=1}^{N} c_i(t_0) e^{\lambda_i(t-t_0)} \mathbf{r}_i \tag{A.7}$$

From the above, it can be observed that the slope trajectory (the rate of a state variable changing) is composed of several behavior modes, each expressed by an eigenvalue and its associated right eigenvector [5]. For nonlinear system, its change rates over a period of time can also be approximated by eigenvalues and eigenvectors.

To express the formula for $\mathbf{x}(t)$, we must deal with the non-homogeneous constant term in Eq. A.2. We proceed Eq. A.2 by rewriting:

$$\dot{\mathbf{x}} = J(\mathbf{x} - J^{-1}\mathbf{b}) \tag{A.8}$$

Suppose $\mathbf{X} = \mathbf{x} - J^{-1}\mathbf{b}$. We have $\dot{\mathbf{X}} = \dot{\mathbf{x}}$. Therefore, we have a homogeneous linear system

$$\dot{\mathbf{X}} = J\mathbf{X} \tag{A.9}$$

The eigenvalue solution of Eq. A.9 is

$$\mathbf{X} = \sum_{i=1}^{N} C_i(t_0) e^{\lambda_i(t-t_0)} \mathbf{r}_i$$

and therefore

$$\mathbf{x} = \sum_{i=1}^{N} C_i(t_0) e^{\lambda_i(t-t_0)} \mathbf{r}_i + J^{-1}\mathbf{b} \tag{A.10}$$

We note that the constant term does not affect the behaviors (eigenmodes) of the system. For our eigenspace analysis at a particular point of time with a small time interval in our study, this constant term can be neglected because the interventions of parameters based on eigenvalue elasticities aim to alter behavior patterns, as captured by eigenvalues. Therefore, in following sections, we do not take the constant terms into consideration.

Table A.1: Eigenvalue classes and corresponding behavior modes.

Eigenvalue Class	Behavior Mode
0	Constant
$a + 0 \cdot i, a > 0$	Exponential Divergent Growth
$a + 0 \cdot i, a < 0$	Exponential Convergent Decay
$0 \pm b \cdot i, b \neq 0$	Sustained Oscillation
$a \pm b \cdot i, a > 0, b \neq 0$	Divergent Oscillation
$a \pm b \cdot i, a < 0, b \neq 0$	Convergent Oscillation

A.2 Eigenmodes of Linear Systems

For a linear system, eigenvalues of its system matrix correspond to elemental behavior modes of the system, and the overall behavior of the system is a superposition of these elemental behavior modes. Table A.1 presents six forms of eigenvalues of a linear system and their corresponding behavior modes. When the imaginary part of an eigenvalue is zero and the real part is nonzero, i.e., in exponential growth or decay mode, the inverse of the real part is the time constant of growth or the negative inverse of real part is the time constant of decay. When both the imaginary and real parts of the eigenvalue are nonzero, the observed frequency of oscillation equals to the absolute value of the imaginary parts of the eigenvalues, and when the behavior mode is convergent oscillation, such a frequency is called the damped frequency [4].

Because the total system behaviors are determined by the superposition of all the eigenmodes, it becomes more difficult to study all eigenvalues when the size of state variables of a large complex system grows, and we therefore seek to focus attention on the 'important' eigenvalues. When the real parts of all eigenvalues of a linear system are negative, the magnitude of variations in system behaviors will die away and the system eventually approaches equilibrium. If not all eigenvalues are negative, the eigenvalue with the largest real part will also eventually dominate the system behaviors [4]. Therefore, we term the eigenvalue with the largest real part the 'dominant eigenvalue' of the system, as it will determine the behavior mode of a linear system. In this study, we assume that there is a unique dominant eigenvalue, and if the dominant eigenvalue is complex we treat that conjugate pair of complex eigenvalues as the same dominant eigenvalue.

With an eye towards identifying these 'important' eigenvalues, we define dominant eigenvectors

as the following.

Definition A.1. For a linear system

$$\dot{\mathbf{x}}(t) = A\mathbf{x}(t)$$

where A is the constant system matrix, its general solution [3] is

$$\mathbf{x} = \sum_i c_i \mathbf{r_i} e^{\lambda_i t}$$

Where c_i are constants and are called the **coefficient**s of the eigenvectors $\mathbf{r}_i$. The eigenvalue with the largest real part is called the **dominant eigenvalue**, and its corresponding eigenvector is termed the **dominant eigenvector**.

For a nonlinear continuous system, the linearization of it in the immediate vicinity period of the point around which the linearization is performed is adequate to describe system behaviors in that period of time [4]. Therefore, in the short term[5], the superposition of eigenmodes of the Jacobian matrix approximates the observed behavior of the nonlinear system in a particular time period. The dominant eigenvalue and eigenvector, as well as its coefficient, together determine the most important behavior mode of the nonlinear system in this period.

---

[5]The time constant associated with "short term" will depend on the the particulars of the system, and specifically, on the speed with which the system's Jacobian evolves.

Appendix B   Detailed Eigenvalue Elasticity Analysis

In this section, we listed the comparisons of simulation results of the individual-based viral dynamic model of 3 persons with changed parameters based on our eigenvalue elasticity analysis.

B.1   Eigenvalue Elasticity with Respect to ω

Fig. B.1 is the comparison of the value of average v across the population with 10% decrement of ω at three time points (each associated with the red, green and grey curve respectively), and the blue curve is the original value of average v in the population. Due to small values of elasticities (on the order of magnitude 10^{-7}), the change of behavior from the perturbation is not significant and is hard to observe in Fig. B.1. Locally between $time = 148$ and $time = 156$, the oscillation of average v is a bit delayed with perturbation of ω at $time = 0.03$ or $time = 10$.
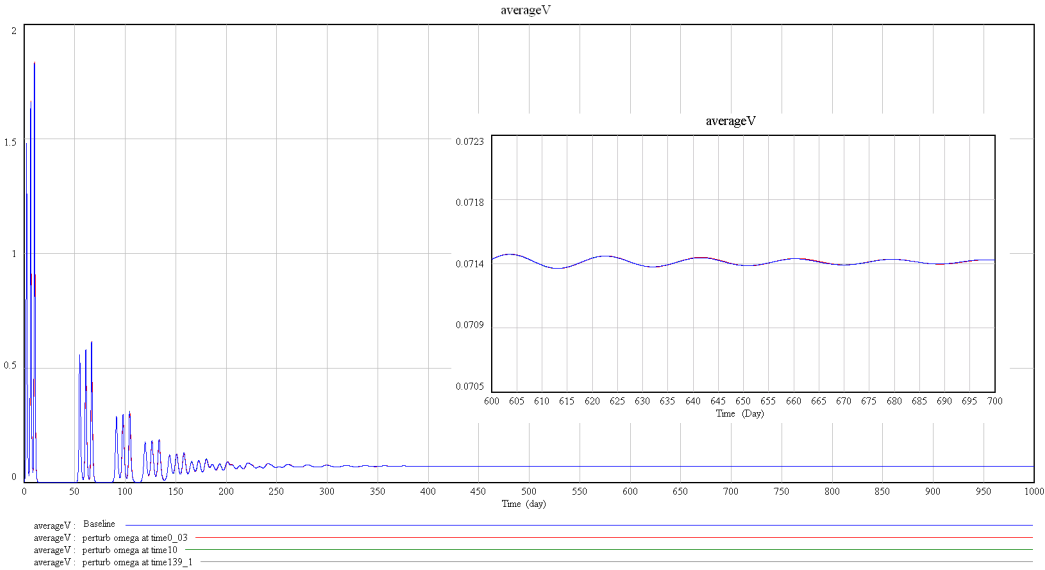
Figure B.1: The value of average v in the population with a small perturbation of ω (the connection weight) at $time = 0.03$, $time = 10$, and $time = 139.1$ respectively for an individual-based viral dynamic model with 3 persons and its local view.

Fig. B.2 is a global view of the behavior of the value of average v across the population overtime with 90% decrement of ω. As shown in the local view of Fig. B.2, during the period from $time = 148$ to $time = 156$, the value of the average v in the population is a bit larger with perturbations than the original one, but the oscillations are delayed. Particularly, the perturbation at $time = 0.03$ has a longer delay of oscillation compared with the original curves than that at $time = 10$ because of the

larger value of the elasticity. But this figure does not clearly show the influence of the perturbation at $time = 139.1$.

Table B.1: The value of average v in population with perturbations of ω at different time for an individual-based viral dynamic model with 3 persons.

	average v in the population				
Time (Day)	148	148.125	148.375	148.5	148.625
Baseline	0.0433	0.0488	0.0490	0.0516	0.0547
perturbed at $time = 0.03$	0.0246	0.0241	0.0235	0.0235	0.0237
perturbed at $time = 10.0$	0.0277	0.0275	0.0278	0.0283	0.0291
perturbed at $time = 139.1$	0.0433	0.0488	0.0490	0.0516	0.0547

Table B.1 gives the value of average v in the population at a selected set of time points. In this table, the perturbation of ω at $time = 139.1$ nearly has no effect on the value of average v, i.e., such perturbation does not apparently change the system behavior.

B.2 Eigenvalue Elasticity with Respect to c

Fig. B.3 is the comparison of the value of average v with perturbations of c at three different time points and its local view from $time = 600$ to $time = 700$, presenting by red, green and grey curves respectively, and the blue curve is the original value of average v in the population.

Table B.2: The value of average v in the population shortly after perturbations of c at different time for an individual-based viral dynamic model with 3 persons.

	average v in the population				
Time (Day)	10.0078	10.0391	10.0703	10.1016	10.1328
Baseline	1.47217	1.56318	1.64619	1.71767	1.77432
perturbed at $time = 10.0$	1.47217	1.56299	1.64507	1.71432	1.76699
proportional changes	0	-1.2155×10^{-4}	-6.8036×10^{-4}	-0.002	-0.004
Time (Day)	94.5859	94.6172	94.6484	94.6797	94.7109
Baseline	0.0222304	0.0219134	0.0216387	0.0213912	0.0211761
perturbed at $time = 94.58$	0.0222304	0.0219134	0.0216386	0.0213911	0.0211758
proportional changes	0	0	-4.6213×10^{-6}	-4.6748×10^{-6}	-1.4167×10^{-5}
Time (Day)	158.727	158.773	158.813	158.852	158.898
Baseline	0.122342	0.121043	0.119902	0.118709	0.117216
perturbed at $time = 158.72$	0.122341	0.121039	0.119889	0.118681	0.117162
proportional changes	-8.1738×10^{-6}	-3.3046×10^{-5}	-1.0842×10^{-4}	-2.3587×10^{-4}	-4.6069×10^{-4}
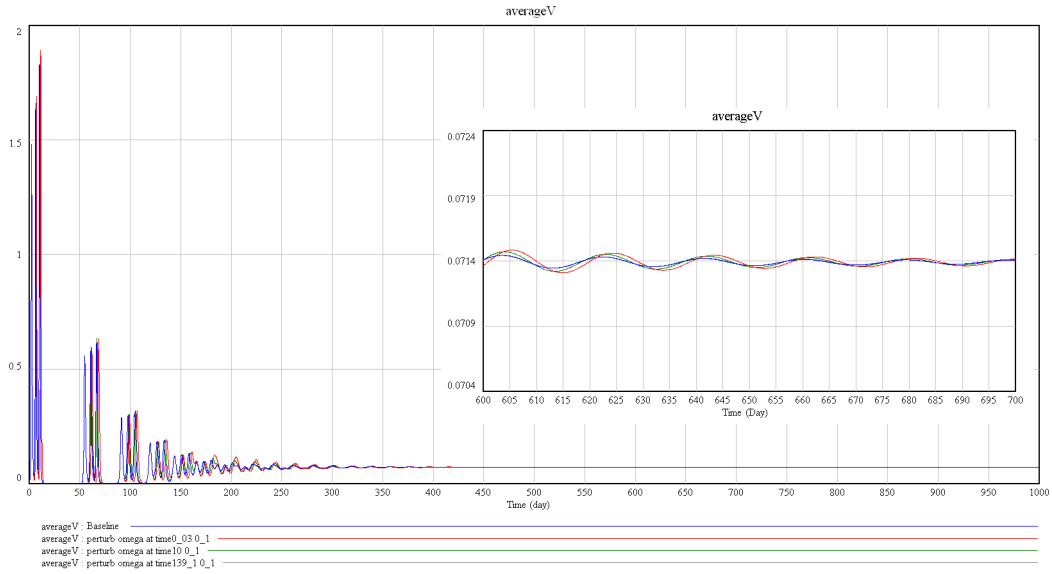
(a) Overall view and local view in the long run
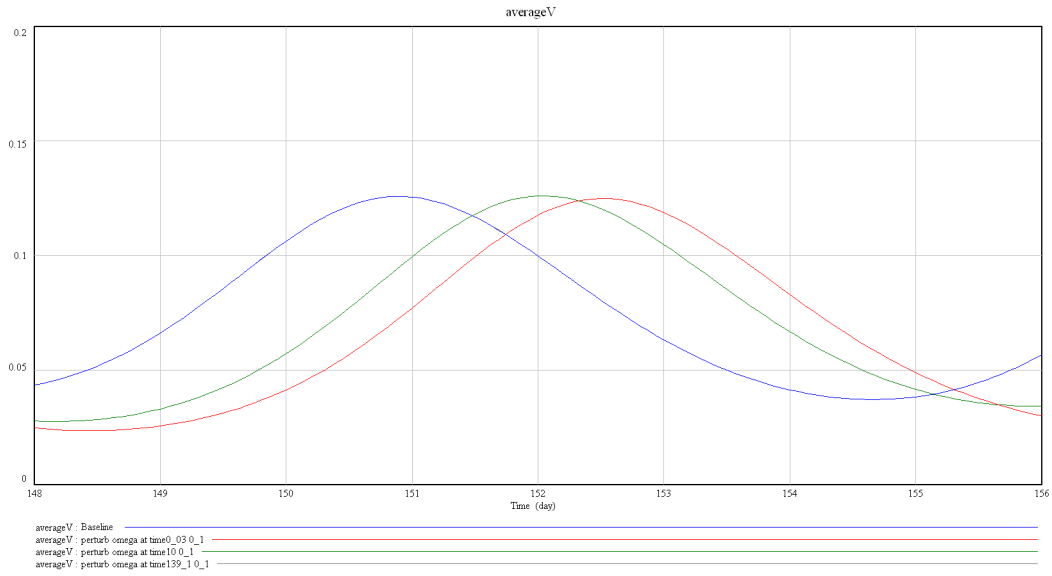
(b) Local view between $time = 148$ and $time = 156$

Figure B.2: The value of average v in population with a large perturbation of ω (`the connection weight`) at $time = 0.03$, $time = 10$, and $time = 139.1$ respectively for an individual-based viral dynamic model with 3 persons and its local views.
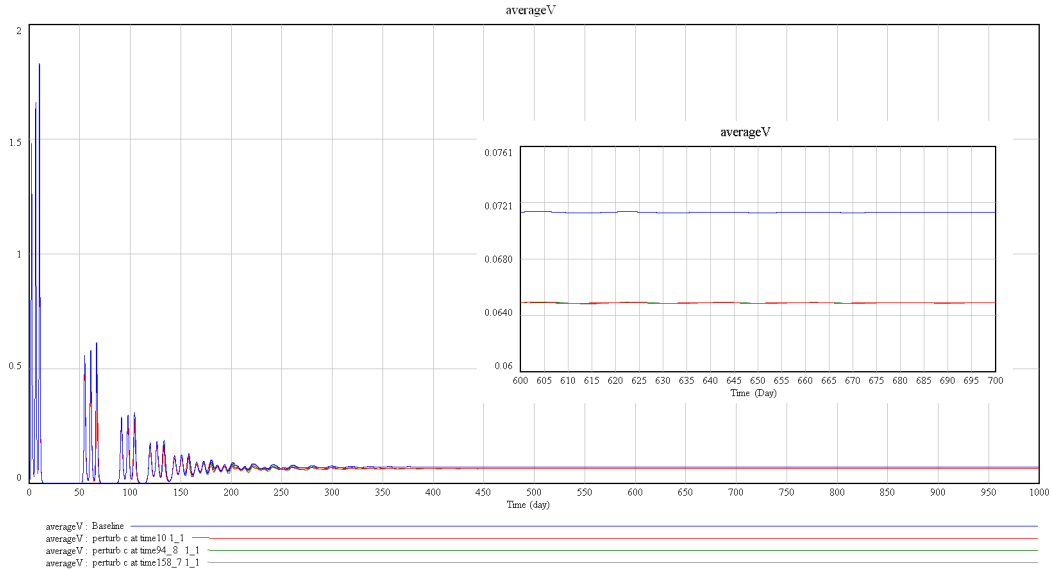
Figure B.3: The value of average v in the population with a perturbation of c (`the production rate of CTL`) at $time = 10$, $time = 94.85$, and $time = 158.72$ respectively for an individual-based viral dynamic model with 3 persons and its local view.

Table B.2 illustrates the local changes of the average v shortly after the perturbation of c. From these simulation results, we could observe that the proportional changes of the average v brought by the perturbation at $time = 158.72$ (when the elasticity is high) is a bit more significant than that from the perturbation at $time = 94.85$ (when the elasticity is lower than that at $time = 158.72$).

Appendix C   Eigenvectors of an Individual-based Viral Dynamic Model with 4 Persons

The row vectors of the matrix below are eigenvectors of the Jacobian matrix at $time = 0.5$ for the individual-based viral dynamics model with four people in Section Section 4.1.2, where `Person 3` and `Person 4` are identical.

0.00000093964	-0.0000010974	0.000044936	0.000000077934	-0.020881	0.046578	-0.99856	-0.016538	-4.2284×10^{-11}	4.9385×10^{-11}	-0.0000000020221	-3.5068×10^{-12}	-4.2284×10^{-11}	4.9385×10^{-11}	-0.0000000020221	-3.5068×10^{-12}
-0.018522	0.022400	-0.73577	-0.0019130	-0.0000041605	0.0000012390	-0.000016527	-0.000000052903	0.012035	-0.014554	0.47806	0.0012429	0.012035	-0.014554	0.47806	0.0012429
-0.017020	0.020584	-0.67608	-0.0017579	-0.0000038225	0.0000011383	-0.000015184	-0.0000048608	-0.013098	0.015840	-0.52027	-0.0013527	-0.013098	0.015840	-0.52027	-0.0013527
0.0000013857	0.0000011112	0.000042395	-0.0000011457	-0.30379	-0.039856	-0.92946	0.20552	-6.3245×10^{-12}	-5.0692×10^{-12}	-1.9349×10^{-11}	5.2286×10^{-12}	-6.3242×10^{-12}	-5.0692×10^{-12}	-1.9349×10^{-11}	5.2286×10^{-12}
-1.6884×10^{-12}	4.6473×10^{-13}	-1.5264×10^{-11}	-4.0157×10^{-14}	-2.2780×10^{-12}	3.5423×10^{-17}	-5.1753×10^{-16}	-2.1919×10^{-16}	-0.017787	0.021511	-0.70655	-0.018370	0.017787	-0.021511	0.70655	0.0018370
-0.11586	0.063511	0.96682	0.026790	-0.0000031400	0.0000075447	0.000026203	0.0000015909	0.018211	-0.0099840	-0.15197	-0.0042101	0.018211	-0.0099840	-0.15197	-0.0042101
-0.025756	0.014120	0.21496	0.0059552	-0.000000069800	0.000000016773	0.000000058256	0.0000000035365	-0.081912	0.044909	0.68364	0.018935	-0.081912	0.044909	0.68364	0.018935
-1.8207×10^{-12}	3.5342×10^{-13}	5.3803×10^{-12}	1.4857×10^{-13}	2.3823×10^{-12}	1.7883×10^{-18}	2.3166×10^{-16}	-3.0318×10^{-15}	0.083912	-0.046006	-0.70033	-0.019398	-0.083912	0.046006	0.70033	0.019398
0.013807	-0.00017236	-0.0034817	-0.99990	0.0000066888	-0.0000000048681	-0.0000016867	-0.0000050974	-0.000000015211	0.000000053805	0.0000000038356	0.0000084810	-0.0000015211	0.0000000053805	0.0000000038356	0.000084810
0.000000057986	-0.000000031174	-0.00000014410	0.0000014634	-0.0096747	0.000011900	0.0024042	-0.99995	0.0000000030939	2.2259×10^{-14}	1.5863×10^{-13}	-5.0865×10^{-11}	-5.7583×10^{-13}	2.2262×10^{-14}	1.5863×10^{-13}	-5.0850×10^{-11}
1.0032×10^{-13}	-1.0885×10^{-14}	-2.4491×10^{-14}	2.3562×10^{-11}	-5.2927×10^{-17}	2.3511×10^{-20}	-1.8387×10^{-20}	-8.4465×10^{-15}	-0.00000021029	0.0000000026023	0.00000052572	0.77478	0.00000017159	-0.000000021235	-0.000000042899	-0.63222
-9.6983×10^{-13}	1.0780×10^{-13}	2.4253×10^{-13}	-0.000000000023334	4.6579×10^{-14}	-2.3496×10^{-19}	1.3916×10^{-19}	8.3829×10^{-15}	0.00000020285	-0.0000000025102	-0.000000050710	-0.74735	0.00000018934	-0.000000022316	-0.000000045084	-0.66443
-1.0	0.0000000051905	0.000000010593	-0.0000000070435	-0.000048737	6.4155×10^{-15}	3.4711×10^{-13}	-4.3708×10^{-13}	0.000038775	-1.3977×10^{-14}	-1.0987×10^{-13}	2.1838×10^{-13}	0.000038766	-1.5977×10^{-14}	-1.0987×10^{-13}	2.1827×10^{-13}
-0.000065976	-1.5529×10^{-14}	-5.9878×10^{-14}	2.1073×10^{-13}	-8.8239×10^{-12}	0.0000000061717	0.000000012595	-0.0000000042047	0.000031391	-3.9754×10^{-19}	-9.3401×10^{-18}	1.7541×10^{-16}	0.000000052785	9.4015×10^{-20}	7.2905×10^{-19}	2.9765×10^{-16}
-0.00000000093861	9.0870×10^{-22}	6.6133×10^{-18}	-1.2331×10^{-20}	-5.4231×10^{-19}	-5.4231×10^{-21}	-1.1054×10^{-19}	3.7024×10^{-19}	-0.014379	2.2448×10^{-16}	4.5812×10^{-15}	-3.0666×10^{-15}	-0.99990	1.5610×10^{-14}	3.1856×10^{-13}	-2.1314×10^{-13}
-0.00000000091112	8.8440×10^{-22}	6.4196×10^{-18}	-1.2006×10^{-20}	-0.00000000050687	-3.1281×10^{-19}	-6.3837×10^{-18}	2.1349×10^{-17}	-0.99988	1.5609×10^{-14}	3.1856×10^{-13}	-2.1314×10^{-13}	0.015298	-2.3882×10^{-16}	-4.8740×10^{-15}	3.2600×10^{-15}